Amyloid β Protein (1−40) Forms Calcium-Permeable, Zn^{2+}-Sensitive Channel in Reconstituted Lipid Vesicles[†,‡]

Hai Lin,* Yinwen Judy Zhu,[§] and Ratneshwar Lal

Neuroscience Research Institute, University of California at Santa Barbara, Santa Barbara, California 93106

Received December 21, 1998; Revised Manuscript Received June 23, 1999

ABSTRACT: Amyloid β protein (AβP) forms senile plaques in the cerebrocortical blood vessels and brain parenchyma of patients with Alzheimer's disease (AD). The nonfamilial or sporadic AD (SAD), the most prevalent form of AD, has been correlated with an increased level of 40-residue AβP (AβP_{1-40}). However, very little is known about the role of AβP_{1-40} in AD pathophysiology. We have examined the activity of AβP_{1-40} reconstituted in phospholipid vesicles. A combined light fluorescence and atomic force microscope (AFM) was used to image the structure of reconstituted vesicles and $^{45}Ca^{2+}$ uptake was used as an assay for calcium permeability across the vesicular membrane. Vesicles reconstituted with fresh and globular AβP_{1-40} contain a significant amount of AβP and exhibit strong immunofluorescence labeling with an antibody raised against the N-terminal domain of AβP, suggesting the incorporation of AβP_{1-40} peptide in the vesicular membrane. Vesicles reconstituted with AβP_{1-40} exhibited a significant level of $^{45}Ca^{2+}$ uptake. The vesicular calcium level saturated over time, showing an important ion channel characteristic. The $^{45}Ca^{2+}$ uptake was inhibited by (i) a monoclonal antibody raised against the N-terminal region of AβP and (ii) Zn^{2+}. However, a reducing agent (DTT) did not inhibit the $^{45}Ca^{2+}$ uptake, indicating that the oxidation of AβP or its surrounding lipid molecules is not directly involved in AβP-mediated Ca^{2+} uptake. These findings provide biochemical and structural evidence that fresh and globular AβP_{1-40} forms calcium-permeable channels and thus may induce cellular toxicity by regulating the calcium homeostasis in nonfamilial or sporadic Alzheimer's disease.

Molecular mechanisms and the cause of Alzheimer's disease (AD)[1] are poorly understood. Alzheimer's disease (AD) is associated with depositions of amyloid β proteins (AβP), 39−43-amino acid peptides, as morphologically heterogeneous neuritic plaques and cerebrovascular deposits (*1*, *2*). These peptides are derived from a proteolytic cleavage of the β-amyloid precursor protein (AβPP), a widely expressed but conserved integral membrane protein with a single membrane-spanning peptide. The subtype and amount of AβP polypeptides vary among various forms of ADs. There is a differential accumulation of AβP_{1-40} and AβP_{1-42} in sporadic Alzheimer's disease (SAD) and nondemented brain samples (*3*), and a mutation in presenilins is linked with an increased ratio of AβP_{1-42} to AβP_{1-40} in familial Alzheimer's disease (FAD) (*4*−*7*). The nonfamilial or sporadic AD (SAD), the most prevalent form of AD, is correlated with an increased level of 40-residue AβP (AβP_{1-40}). However, very little is known about the role of AβP_{1-40} in such pathology and its mechanism(s) of action.

Amyloid β protein plays an early and *causative* role in the AD pathogenic cascade (*8*−*11*). Proposed mechanisms of AβP toxicity include its interaction with cell-surface receptors such as the tachykinin receptors (*12*), changing the cellular ion concentration via plasma membrane channels (*13*−*17*), and activating oxidative pathways and increasing the responsiveness to oxidative stress (for reviews, see refs *18* and *19*). However, the roles of the reactive oxygen mechanism and the tachykinin receptor pathway are indirect and less definitive. Moreover, AβPs of differing sizes associated with the reactive oxygen hypothesis have produced conflicting effects on cytoskeletal organization and cell lysis (*20*−*25*), and the role of the tachykinin neuropeptide pathway in AβP toxicity has been inconsistent.

An altered cellular calcium level is a common denominator underlying AβP toxicity (*17*, *26*−*29*). Such a calcium change could be caused either indirectly via modulating the existing Ca^{2+} channel or directly by AβP-formed channels. AβP_{1-40} elicits cation-selective currents when reconstituted in artificial lipid bilayers (*13*−*15*) and when incubated with membrane patches excised from hypothalamic GnRH neurons (*30*). Low-angle X-ray diffraction studies have shown that AβP_{25-35} is highly lipophilic and spontaneously inserts into the membrane hydrocarbon core (*21*, *31*). Durell et al. (*32*) have proposed theoretical models for the structure of the ion channel formed by the membrane-bound AβP_{1-40}. However, no direct structural data from EM, X-ray diffraction, NMR,

[†] This work was supported by a grant from the Alzheimer's Disease Program, Department of Health, California, and the NIH (NIGMS and NIA).

[‡] Portions of this work appeared as an abstract from the American Society for Cell Biologists 1998 annual meeting.

* To whom correspondence should be addressed: Neuroscience Research Institute, University of California, Santa Barbara, CA 93106. Telephone: (805) 893-2350. Fax: (805) 893-2005. E-mail: h_lin@lifesci.ucsb.edu.

[§] Present address: Molecular Imaging Corp., Phoenix, AZ.

[1] Abbreviations: AβP, amyloid β protein; AD, Alzheimer's disease; APP, amyloid precursor protein; AFM, atomic force microscope.

10.1021/bi982997c CCC: $18.00
Published on Web 08/04/1999

or other microscopic techniques are available to support the presence of the AβP channel. Moreover, other groups have often found conflicting results from electrical recordings (*33*, *34*).

We have used an integrated atomic force and light fluorescence microscope (*35*) and $^{45}Ca^{2+}$ uptake assay (*16*) to examine calcium permeability in lipid vesicles reconstituted with AβP_{1-40}. Commonly used electrical current measurement across lipid membranes often includes contaminating currents when reconstituted with small hydrophobic peptides. $^{45}Ca^{2+}$ uptake measures Ca^{2+} transport across the lipid vesicle bilayer. $^{45}Ca^{2+}$ uptake study is not subjected to such contaminations. Moreover, it allows examination of the dose-response relationship of $^{45}Ca^{2+}$ uptake, and thus, various pharmacological studies are feasible. Consistent with the possibility of fresh AβPs forming ion-permeable channels, we show that (i) AβP incorporates in reconstituted lipid vesicles, (ii) vesicles reconstituted with AβP exhibit a significant level of $^{45}Ca^{2+}$ uptake which is blocked by anti-AβP antibody and Zn^{2+}, but not blocked by an antioxidant, and (iii) the kinetics of calcium uptake is consistent with that of ion channel activity.

EXPERIMENTAL PROCEDURES

Materials. 1,2-Dioleolyl-*sn*-glycero-3-phosphatidylethanolamine (DOPE) and 1,2-dioleolyl-*sn*-glycero-3-phospho-L-serine (DOPS) were obtained from Avanti Polar Lipids (Alabaster, AL). Synthetic β-amyloid$_{1-40}$ peptide was purchased from Bachem (Torrance, CA) and also obtained from Y. Hirakura (University of California, Los Angeles, CA) which was synthesized at Yale University (New Haven, CT). A monoclonal antibody against the N-terminus of AβP [3D6, anti-AβP 1−5 (DAEFR)] was kindly provided by R. Rydel at Athena Neurosciences, Inc. (South San Francisco, CA). Goat anti-mouse IgG conjugated with cy3 was purchased from Jackson Immuno Research Laboratories (West Grove, PA). AβP_{1-40} was dissolved in H_2O at a concentration of 5 mg/mL and stored at −20 °C. Before use, AβP_{1-40} was thawed and bath sonicated for 5 min to break up any cluster formation.

Liposome Preparation. Equal portions of DOPE and DOPS (10−25 mg/mL) in chloroform were mixed together and dried under a stream of argon gas, and the organic solvent residue was removed by vacuuming with a speed vac for 1 h. Dried lipids were resuspended in a 20 mM Hepes (pH 7.4) aqueous solution at a concentration of 1.11 mg/mL. The lipid mixture was bath sonicated for 20 min. To reconstitute AβP into liposomes, 1 part of AβP (5 mg/mL) was mixed with 9 parts (volume) of the lipid mixture and bath sonicated for 20 min. To obtain the control liposomes without AβP, $^1/_9$ of a volume of H_2O was added to the lipid mixture and bath sonicated for 20 min. The final liposome buffer contains 20 mM NaHepes (pH 7.40) and 1 mg/mL lipids (1:1 DOPS/DOPE); the AβP concentration was 0.5 mg/mL.

The percentage of AβP incorporation in liposomes was estimated with a method described by Mason et al. (*31*). Briefly, liposomes reconstituted with AβPs were centrifuged at 35000*g* for 90 min at 5 °C. The relative AβP contents in the pellets (liposome) and supernatant were measured with the amido black dye binding protein assay. To ensure that the measured AβP content was associated with liposomes and not unassociated large AβP aggregates, 20 mM Hepes buffer containing the same amount of AβP without lipid was centrifuged in parallel to determine the quantity of unincorporated AβP in the pellet. Very little of the AβP dissolved in aqueous buffer was sedimented (less than 0.5%) after centrifugation for 90 min at 35000*g*, indicating that little soluble AβP formed very large aggregates.

Immunolabeling with Anti-AβP Antibody. Liposomes reconstituted with or without AβPs as well as buffer containing only soluble AβPs were centrifuged at 35000*g* for 90 min at 5 °C (very little AβPs was pelleted from buffer containing only soluble AβPs). Pellets were rinsed and resuspended in 20 mM Hepes, and portions of each sample were deposited on glass coverslips for 20 min followed by rinses with phosphate-buffered saline (PBS, Life Technologies, Rockville, MD) and fixation for 10 min with 4% paraformaldehyde. Each sample was washed with PBS and with PBS containing 3% bovine serum albumin (BSA) and 1% goat serum. The samples were incubated with 3D6 anti-AβP antibody in PBS (2 μg/mL) containing 3% BSA and 1% goat serum, for 1 h at room temperature. After washing with PBS, the sample was incubated with cy3-conjugated goat anti-mouse IgG (1:500 dilution) under the same condition that was used for primary antibody incubation. Fluorescence images were captured using 60× objective lenses with a Bio-Rad MRC-1024 laser confocal microscope.

Imaging Liposomes with Atomic Force Microscopy. AFM images were obtained as previously described (*16*) using a prototype of Bioscope AFM (*36*) and a Multimode AFM (Digital Instruments, Santa Barbara, CA). A contact mode AFM was used for most of the images. Oxide-sharpened silicon nitride tips with a nominal spring constant of about 0.06 N/m (Digital Instruments) were used for most of the experiments. All AFM imaging was conducted on liposomes in aqueous solutions. For liposomes reconstituted with or without AβP_{1-40}, 20−50 μL of liposomes was absorbed on a clean glass coverslip or glass Petri dish or freshly cleaved mica for 30 min. The substrate was then rinsed with a buffer [20 mM Hepes (pH 7.4)] and imaged in the buffer. The imaging force was regularly monitored and kept to a minimum, unless specified. The imaging force generally varied from a sub-nanonewton (nN) to tens of nanonewtons. All imaging was performed at room temperature (22−24 °C). The liposomes were also imaged in deionized water as described previously (*16*).

Measurement of the Rate of $^{45}Ca^{2+}$ Uptake into Liposomes. The $^{45}Ca^{2+}$ uptake assay was based on a method previously described (*16*). Briefly, 25 μL of liposomes reconstituted with or without AβP_{1-40} was incubated with 75 μL of a buffer containing 20 mM Hepes (pH 7.4), 0.5 mM Ca^{2+}, and 1 μCi of $^{45}Ca^{2+}$ for a specific period of time, at room temperature. For each sample, $^{45}Ca^{2+}$ uptake was stopped with 300 μL of blocking buffer containing 10 mM Tris-HCl (pH 7.4), 20 mM $ZnCl_2$, 0.5 mM $CaCl_2$, and 15 μg/mL 3D6 antibody. The 400 μL mixture of liposomes and the blocking buffer was promptly loaded onto a Chelex 100 column (Bio-Rad, Hercules, CA; bead volume of 3 mL) which had been pre-equilibrated with a buffer containing 200 mM sucrose, 20 mM Tris-HCl (pH 7.4), and 0.3% BSA. The liposomes were immediately eluted from the column with 5 mL of a buffer containing 200 mM sucrose and 20 mM Tris-HCl (pH 7.4).

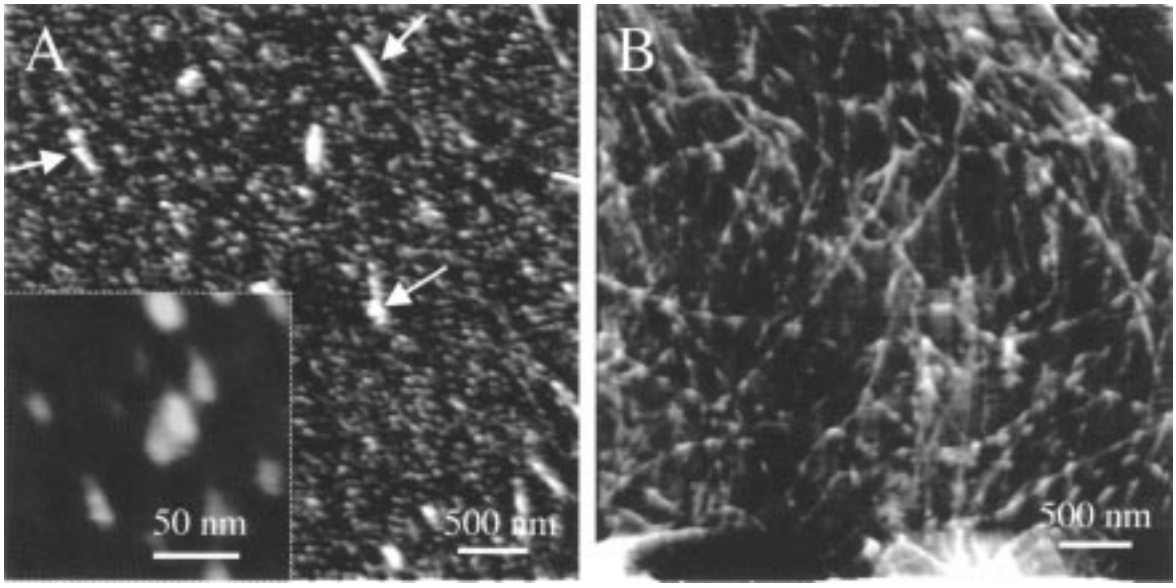

FIGURE 1: Images of fresh and aged AβP$_{1-40}$ produced with an AFM. AFM height mode images (surface plot) of AβPs adsorbed on mica and imaged in PBS. (A) Image of fresh AβP$_{1-40}$ absorbed on mica. Primarily, globular AβPs with a few short fibrils (denoted by the arrows) are present. The average size of the individual globules is 8−10 nm, though larger conglomerates are also visible. The inset gives an enlarged view of some globular aggregates. No attempt was made to discern the high-resolution structure of individual subunits. (B) Image of aged AβP$_{1-40}$ (after incubation for 24 h), where long fibrils are present.

Fractions (0.1−0.2 mL) of the eluted liposome containing buffers were counted with a Beckman liquid scintillation counter to determine the relative $^{45}Ca^{2+}$ content of the liposomes.

To confirm that the saturation level of intravesicular $^{45}Ca^{2+}$ had equilibrated with the external $^{45}Ca^{2+}$ level, the intravesicular $^{45}Ca^{2+}$ level after a prolonged period (>10 min) of uptake was compared with the internal $^{45}Ca^{2+}$ level in liposomes reconstituted in the presence of AβPs and 1 μCi of $^{45}Ca^{2+}$. This also provides a good estimate of the total internal volume of the liposomes, by comparing the $^{45}Ca^{2+}$ counts in the liposomes versus the total $^{45}Ca^{2+}$ counts in the buffer.

RESULTS

AFM Imaging of AβPs. The structural conformation of AβP such as globular versus fibrillar is reported to correlate with AβP toxicity. We imaged fresh as well as aged AβP$_{1-40}$ adsorbed on a freshly cleaved mica surface with an AFM in aqueous solutions. AFM images of freshly prepared AβPs reveal the presence of both small particles with an average diameter of 1−2 nm and larger globular aggregates with an average diameter of 8−10 nm. Figure 1A shows representative larger globular aggregates with a nominal size of 8−10 nm. No attempt was made to image the fine structure in these globular aggregates, but they could potentially form AβP channels and exhibit ion channel-like activity when incorporated into a lipid bilayer. Freshly prepared AβPs also contain a very small percentage of 200−300 nm short fibers (less than 1%) as indicated by the arrows in Figure 1A. In contrast to the AFM images of fresh AβPs, AFM images of aged AβPs (AβPs stored for ≥24 h at room temperature) revealed a mixed population of mostly long fibrous strands (>90%) and some small globular particles (Figure 1B).

AFM Imaging of Liposomes and Immunolocalization of AβP in Reconstituted Liposomes. Liposomes reconstituted with or without AβP$_{1-40}$ were imaged with an AFM. Morover, to examine whether AβP$_{1-40}$ was incorporated in reconstituted liposomes, we examined immunofluorescence labeling of liposomes reconstituted with or without AβP$_{1-40}$ and quantified the content in the reconstituted vesicles with a quantitative protein assay.

Liposomes reconstituted with AβPs have a well-defined vesicular structure as revealed by AFM imaging (Figure 2A−C). Vesicles reconstituted without AβPs are smaller but more spherical compared to the vesicles reconstituted with AβPs. Vesicles reconstituted with AβP ranged mostly in size from approximately 0.2 to 0.5 μm in diameter, with a few larger vesicles up to 1.0 μm in diameter. The larger vesicles were often flattened in a disk shape. The vesicular flattening and larger size are probably due to the protein−lipid interactions as is the case with other membrane proteins such as gap junctions and acetylcholine receptors (*37*, *38*). The height of the flattened vesicles was between 20 and 30 nm, which is typical for unilamellar vesicles composed of upper and bottom lipid bilayers (*39*). When imaged with a higher imaging force, which can be used to dissect away the upper bilayer, the AFM images of vesicles clearly showed that the vesicles were bound by a single lipid bilayer wall (Figure 2C).

The quantitative protein assay showed that after reconstitution, 15 ± 1% (n = 3, mean ± standard error of the mean) of all AβP was associated with the liposomes, suggesting the incorporation of AβP in the liposomes.

Liposomes reconstituted with or without fresh AβP$_{1-40}$ were also immunolabeled with an anti-AβP antibody (3D6). Figure 3A shows immunolabeling of liposomes reconstituted with AβP$_{1-40}$. On the other hand, little immunolabeling was observed in samples prepared from resuspended pellets of AβP$_{1-40}$ (Figure 3B), which is not surprising since very little AβP was sedimented by centrifugation (<0.5%). There was also no immunofluorescence observed in liposomes reconstituted without AβP$_{1-40}$ (Figure 3C). These results indicate that AβP$_{1-40}$ is incorporated in the liposome membrane. We

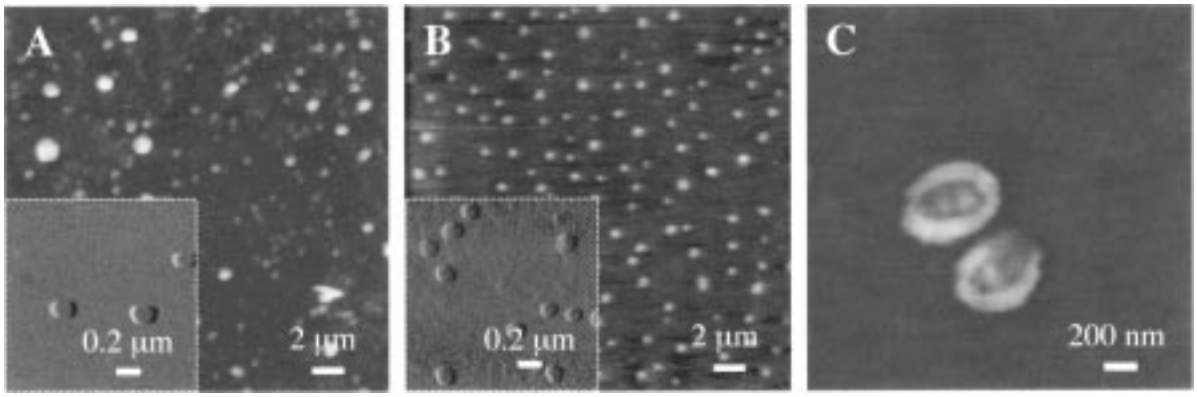

FIGURE 2: AFM images of reconstituted vesicles. Height mode images of DOPS/DOPE liposomes prepared by bath sonication, reconstituted (A) with or (B) without AβP. Insets in panels A and B show closeup error mode AFM images of representative liposomes with or without AβP, respectively. Panel C is a height mode image of liposomes reconstituted with AβP_{1-40} imaged with a higher imaging force, a force which can be used to dissect the upper vesicular bilayer. The vesicles are clearly unilamellar and surrounded by a single bilayer. The thickness of a single bilayer is approximately 6 nm.

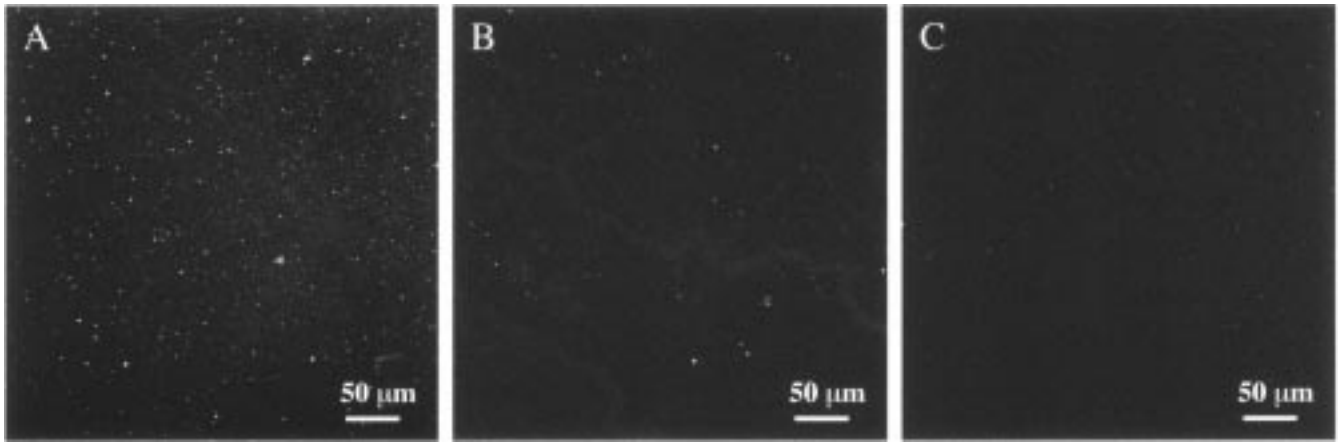

FIGURE 3: Confocal images of reconstituted liposomes fluorescently immunolabeled with anti-AβP antibody 3D6. Liposomes reconstituted with and without AβP_{1-40} as well as soluble AβP were centrifuged, and pellets were resuspended and absorbed onto glass coverslips for immunolabeling. (A) Liposomes reconstituted with AβP_{1-40} exhibit punctate immunofluorescence labeling for AβP. Little immunolabeling was observed in samples of either resuspended sediment of centrifuged soluble AβP_{1-40} (B) or liposomes reconstituted without AβP_{1-40} (C). All three images are projections from multiple vertical optical sections. A strong fluorescence signal suggests that there could be a large amount of AβP incorporated in the vesicles, although the brightness (and the spatial dimension) of the fluorescence signal depends on several factors, including the number of fluorophores and antibodies and the amount and conformations of AβP molecules.

also examined whether fibrillar AβPs are reconstituted in the lipid vesicles. Strikingly, no significant level of immunolabeling was observed in the vesicles reconstituted with aged AβPs, suggesting a lack of any incorporation into lipid vesicles (data not shown).

AβP Channel-Specific Calcium Uptake. Liposomes reconstituted with AβP_{1-40} (Figure 4, ▲) have a level of $^{45}Ca^{2+}$ uptake that is 6−10 times higher than that of liposomes reconstituted without AβP_{1-40} (Figure 4, ●). The extent of $^{45}Ca^{2+}$ uptake by liposomes reconstituted with fresh AβP_{1-40} exhibits a time-dependent saturating pattern (Figure 4, ▲), consistent with the channel-like activity of reconstituted AβPs. The higher level of $^{45}Ca^{2+}$ uptake is not caused by the direct binding of $^{45}Ca^{2+}$ to incorporated AβP peptides or AβP−lipid molecule complexes since AβP_{1-40} alone (without any lipids) did not exhibit any significant $^{45}Ca^{2+}$ radioactivity (Figure 4, ■). $^{45}Ca^{2+}$ uptake is partially inhibited by a monoclonal antibody (3D6, 20 μg/mL) raised against the N-terminal region of AβP (Figure 4, ⬡), showing that the level of $^{45}Ca^{2+}$ uptake is AβP-specific. Furthermore, liposomes reconstituted with bovine serum albumin alone (without AβPs) did not exhibit any significant $^{45}Ca^{2+}$ uptake above the levels observed for the liposomes reconstituted with lipids alone (data not shown).

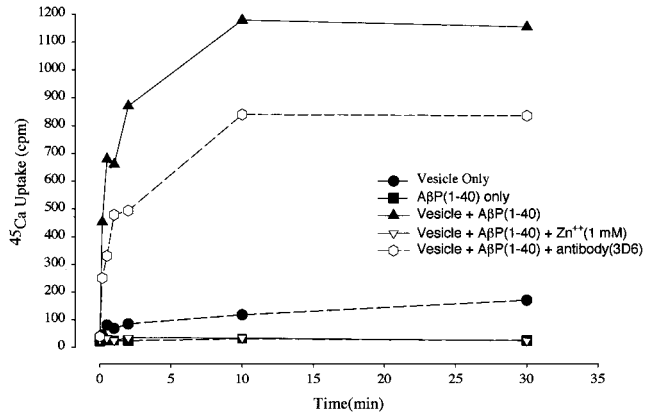

FIGURE 4: Time-dependent uptake of $^{45}Ca^{2+}$ under different conditions: $^{45}Ca^{2+}$ uptake in liposomes reconstituted with lipids only (●) and liposomes reconstituted with AβP_{1-40} (▲). $^{45}Ca^{2+}$ uptake in liposomes reconstituted with AβP_{1-40} was partially inhibited by an anti-AβP monoclonal antibody (3D6, 20 μg/mL) (⬡) and completely blocked by 1 mM Zn^{2+} (▽). In the absence of lipids, AβP_{1-40} (0.5 mg/mL) alone did not bind to $^{45}Ca^{2+}$ (■).

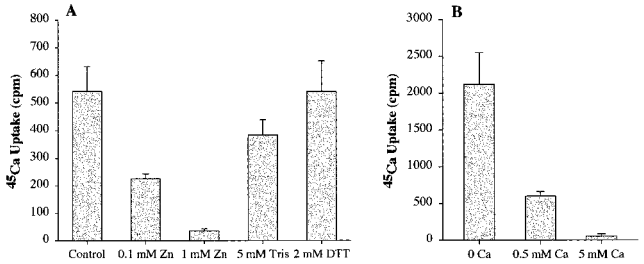

FIGURE 5: $^{45}Ca^{2+}$ uptake into liposomes reconstituted with AβP$_{1-40}$. (A) Level of $^{45}Ca^{2+}$ uptake after incubation for 2 min under control conditions and in the presence of 0.1 mM Zn^{2+}, 1 mM Zn^{2+}, 5 mM Tris, or 2 mM dithiothreitol. (B) Level of $^{45}Ca^{2+}$ uptake after incubation for 1 min in the presence of 0, 0.5 (the control condition), and 5 mM nonradioactive Ca^{2+}. The data in these graphs are the average of triplicate samples, and the error bars represent the standard error of the mean.

To ensure that all liposomes reconstituted with AβP took up $^{45}Ca^{2+}$ and the saturation $^{45}Ca^{2+}$ level in reconstituted liposomes reached equilibrium with the external $^{45}Ca^{2+}$ level, we measured the $^{45}Ca^{2+}$ level in vesicles reconstituted in the presence of 1 μCi of external $^{45}Ca^{2+}$. Under such a condition, the concentration of $^{45}Ca^{2+}$ in the vesicles should be the same as the $^{45}Ca^{2+}$ concentration in the external buffer. For a normalized liposome concentration (1 mg/mL phospholipid), the amount of $^{45}Ca^{2+}$ in vesicles reconstituted in external $^{45}Ca^{2+}$ was 2.1 $\pm$ 0.3% ($n = 4$) of the total $^{45}Ca^{2+}$ in the buffer, which is not statistically significantly different from the saturation levels of $^{45}Ca^{2+}$ uptake in liposomes reconstituted with AβP. In a paired experiment, after incubation for 30 min in the $^{45}Ca^{2+}$ buffer, the amount of $^{45}Ca^{2+}$ in vesicles reconstituted in the absence of external $^{45}Ca^{2+}$ was 1.7 $\pm$ 0.3% ($n = 4$) of the total $^{45}Ca^{2+}$ in the buffer. These results indicate that the saturation $^{45}Ca^{2+}$ level in liposomes was near equilibrium with the external $^{45}Ca^{2+}$ level in the buffer and essentially all liposomes contained at least one AβP-formed Ca^{2+} channel. These results also give an estimate of the total volume of the vesicles as approximately 2% of the buffer volume, which is typical for unilamellar liposomes (*40*).

We examined the mechanisms of AβP$_{1-40}$-specific calcium uptake. In this study of AβP$_{1-40}$, $^{45}Ca^{2+}$ uptake was blocked by 1 mM Zn^{2+} (Figure 4, ∇), which may also compete against binding of $^{45}Ca^{2+}$ to negatively charged phospholipid headgroups. The $^{45}Ca^{2+}$ uptake in liposomes reconstituted with AβP$_{1-40}$ was not inhibited by DTT (2 mM), an antioxidant (Figure 5A), but was partially inhibited by Tris (5 mM, pH 7.4). Figure 5A summarizes the level of $^{45}Ca^{2+}$ uptake by liposomes reconstituted with AβP$_{1-40}$ after incubation for 2 min with $^{45}Ca^{2+}$ in the presence of (i) 0.1 mM Zn^{2+}, (ii) 1 mM Zn^{2+}, (iii) 5 mM Tris (pH 7.4), and (iv) 2 mM DTT. Moreover, $^{45}Ca^{2+}$ uptake is competitively inhibited by increasing the concentration of nonradioactive Ca^{2+}. Figure 5B summarizes the level of $^{45}Ca^{2+}$ uptake in liposomes after incubation for 1 min in buffers containing (i) 0, (ii) 0.5 mM (control), and (iii) 5 mM nonradioactive Ca^{2+}. The data points in these graphs are the averages of triplicate samples for each point, and the error bars represent the standard error of the mean.

DISCUSSION

We have examined functional properties of AβP$_{1-40}$ reconstituted in lipid vesicles using complementary techniques of atomic force microscopy, light immunofluorescence microscopy, and $^{45}Ca^{2+}$ uptake. Vesicles reconstituted with fresh and globular AβP$_{1-40}$ contain a significant amount of AβPs and exhibit strong immunofluorescence labeling with an antibody raised against the N-terminal domain of AβP, suggesting the incorporation of AβP$_{1-40}$ in the vesicular membrane. Vesicles reconstituted with AβP$_{1-40}$ exhibited a significant level of $^{45}Ca^{2+}$ uptake that saturated over time, an important ion channel characteristic. The $^{45}Ca^{2+}$ uptake was inhibited by (i) a monoclonal antibody raised against the N-terminal region of AβP and (ii) Zn^{2+}. However, a reducing agent (DTT) did not inhibit the $^{45}Ca^{2+}$ uptake, indicating that the oxidation of AβP or its surrounding lipid molecules is not directly involved in the AβP-mediated Ca^{2+} uptake.

AFM Imaging of Isolated AβPs. AFM images of freshly prepared AβP$_{1-40}$ show the presence of both small particles with an average diameter of 1−2 nm and larger globular aggregates with an average diameter of 8−10 nm. The small diameter particles may represent monomeric and dimeric AβP polypeptides. The larger globular aggregates with an average size of 8−10 nm could represent the channel-forming portion of AβPs and exhibit ion channel-like properties after proper incorporation into a lipid bilayer. Such a globular size is consistent with the size of AβP channels as proposed in the model of its three-dimensional structure (*32*). The model predicts channels to be made of four to eight monomeric subunits and is supported by electrical measurements in reconstituted bilayer studies (*13*−*15*, *34*). In the study presented here, we did not intend to decipher the channel-like structural arrangement of the globular AβPs; such study will require extensive and sub-nanometer resolution structural examination of reconstituted vesicles with AβPs.

Roher et al. (*41*) have recently imaged AβP$_{1-42}$ with an AFM and showed granular ellipsoidal particle aggregates with average size of 3−4 or 7−8 nm and with occasional aggregation into larger conglomerates. The average size difference of AβP$_{1-42}$, the 3−4 nm diameter as observed by Roher et al. (*41*) versus the 1−2 nm diameter observed in our study, may reflect the differences in the imaging conditions [hydrated AβPs imaged in PBS in our study vs dry AβPs imaged in 2-propanol and air in the study by Roher et al. (*41*)] and/or the difference in the packing of residues 1−40 and 1−42 of AβPs. Fresh AβPs, negatively stained and imaged with an EM, were globular particles with an average diameter of 30 nm (*24*). In our AFM studies, though the smaller particles (2−10 nm) predominate, a few particles with a larger diameter were also apparent. Such a distribution of particle size as observed by AFM and EM studies may reflect the varying degrees of constraints imposed on sample preparations and imaging by these techniques; AFM imaging requires very little sample preparation, and the imaging is less invasive. Aged AβPs exhibit fiber-like features with some globular structures. Previous EM images of aged AβPs exhibit similar fiber-like structures (*24*). Significantly though, in that study, all samples derived from the populations with high toxicity contained small globular AβP particles.

AβP in Reconstituted Liposomes. Our protein assay experiment provides evidence that AβP$_{1-40}$ was incorporated in the liposomes, though the rate of incorporation was lower than that of AβP$_{25-35}$ (*31*). In addition, anti-AβP antibody immunolabeling was observed on vesicles reconstituted with

AβP$_{1-40}$, but not in vesicles reconstituted without AβP$_{1-40}$ or in isolated AβP$_{1-40}$ adsorbed to the substrate (Figure 3). The site-directed antibody used in our study is specific to the extramembranous amino terminus portion of the AβP polypeptide. Thus, the immunolabeling results suggest that the amino-terminal portion of the AβP polypeptide is exposed to the exterior of the lipid vesicles and the polypeptide is not entirely encapsulated in the aqueous interior of liposomes. This is consistent with the results of the low-angle X-ray diffraction study of AβP$_{25-35}$ and lipid membrane interaction (*31*), which showed that AβP$_{25-35}$ is highly lipophilic and spontaneously intercalates into the membrane bilayer and suggested that peptide residues 29−35 are imbedded in the hydrocarbon core of the lipid bilayer.

Recently, Choo-Smith et al. (*42*) have reported a requirement for the presence of gangliosides for the interaction of AβP with vesicles containing zwitterionic or acidic phospholipids. We have not systematically examined AβPs reconstituted in zwitterionic phospholipids. Our results from the $^{45}Ca^{2+}$ uptake assay and immunolabeling of AβPs in liposomes, however, suggest that AβPs can directly interact with negatively charged phospholipids and do not require any gangliosides (*31*). The presence of AβP in phospholipid vesicles is consistent with the possibility of AβP$_{1-40}$ forming cation-selective channels in membranes (*13*−*15*, *30*). The relatively high level of AβP incorporation in the vesicular membrane is a desirable feature for imaging of AβP channels in the membrane. Further study is underway in an effort to examine the three-dimensional structure of the putative AβP channel.

Since AβPP is a membrane protein, it was believed that the membrane-bound AβP portion would not be found as a free peptide except when there is membrane injury leading to a proteolytic cleavage of AβPP. In addition, it was believed that the self-aggregating and hydrophobic nature of AβP would prohibit it from existing as a soluble, circulating peptide in normal biological fluids. Subsequent studies, however, revealed soluble AβPs being secreted into the conditioned media of a variety of primary or transfected AβPP-expressing cells under normal metabolic conditions (*43*−*45*). Our result and other recent studies (*31*) suggest that the soluble AβPs could directly interact with lipid membrane. Whether they form a channel-like three-dimensional structure is still under investigation, but the increasing evidence suggests the presence of such channels (see the following section).

AβP$_{1-40}$ Channel-Specific Calcium Uptake. Liposomes reconstituted with AβP$_{1-40}$ exhibit a significant level of $^{45}Ca^{2+}$ uptake. The calcium uptake is dose-dependent and exhibits a time-dependent saturation pattern. The calcium uptake was inhibited by zinc, but not by physalaemin and DTT. Recent studies suggest that AβPs of different sizes (i.e., AβP$_{1-42}$, AβP$_{25-35}$, and AβP$_{1-40}$) form cation-selective channels whose activity can be inhibited by zinc, Tris, and other related compounds (*16*). AβP$_{1-40}$-specific cationic channels are reported in AD-free fibroblasts, endothelial cells, and neuronal patches (*26*−*30*), and AβP$_{1-40}$-specific calcium uptake has been reported in AD-free fibroblasts (preliminary results; *17*).

It has recently been shown that AβP binds specifically and saturably with zinc in a biphase mode: high-affinity binding (K_D = 107 nM) and low-affinity binding (K_D = 5.2 μM) (*46*). The zinc-binding site has been mapped to a stretch of contiguous residues between positions 6−28 of the AβP sequence. Zinc, at a concentration of more than 1 mM, facilitates the precipitation of soluble AβP from aqueous buffer (*47*, *48*). This property could be pathologically important because zinc is abundant in the same neocortical regions where AβP deposits are most commonly found. Moreover, the concentration of zinc reaches a high micromolar range during glutamatergic neurotransmission (*49*, *50*), providing one possible explanation for the propensity of AβP to deposit close to the neocortical synaptic vicinity.

An antioxidant (DTT) did not inhibit calcium uptake, which indicates that AβP$_{1-40}$-dependent $^{45}Ca^{2+}$ uptake is not due to the oxidation of the AβP$_{1-40}$ peptide (*12*). Antioxidants presumably interact with the membrane lipid components and change the membrane permeability (for reviews, see refs *16*−*18*). Our results strongly suggest that the antioxidants have little or no effect on AβP$_{1-40}$ channel-mediated ionic exchange in vitro. Such a finding is consistent with our recent observation that antioxidants have no effect on calcium permeability through channels formed by AβP$_{1-42}$ (*16*). At the cellular level, AβPs of differing sizes, reported to be associated with the reactive oxygen hypothesis, have produced conflicting effects on the cytoskeletal organization and cell lysis (*20*−*25*). In AD-free aged fibroblasts, Trolox and DTT did not prevent AβP$_{1-40}$-induced cell degeneration (preliminary results; *17*); a similar observation was made in endothelial cells as well (preliminary results; *29*).

For the channel hypothesis to be relevant in cellular toxicity, the efficiency of channel formation should be high. The concentration of AβP$_{1-40}$ for channel formation in our study is very comparable to the concentrations at which others have described channel formation both by AβP$_{1-40}$ and AβP$_{1-42}$ and by other amyloid proteins such as amylin, PRP(106−126) (*13*, *30*, *33*, *51*), and serum amyloid A (*52*), as well as C type naturuetic peptide (*53*), β2 microglobulin, and transthyretin.

Because of the nature of the aggregation process, it is likely that only a small fraction of the total AβP is available for channel formation. Monomeric or very small aggregates [dimers or trimers (*32*)] of AβP probably cannot form channels. Very large aggregates of AβPs probably also cannot form channels. So, it is consistent with what we know about aggregation that only a small percentage of the total protein is available for channel formation.

The concentration of AβP required to form channels is much higher than those required for other channel formers such as colicin or diphtheria toxin. However, it is clear that the amyloid peptides are not proteins designed to be toxins, but rather aberrant proteins with a weak toxic property which nonetheless turns out to be significant under conditions where disease processes lead to abnormal accumulation or perhaps abnormally high concentrations of these proteins.

Although the concentrations of AβP used in reconstitution studies are higher than the physiologic concentration of AβP in cerebrospinal fluid, it is certainly possible that AβP attains higher concentrations in localized areas of affected tissues. Indeed, there is some evidence that AβP accumulation occurs in intracellular compartments such as endosomes and lysosomes (*54*) and could be released under appropriate pathophysiologic conditions. Our preliminary results show that

$A\beta P_{1-40}$ causes a significant increase in the cellular level of free calcium and the eventual cellular degeneration.

In summary, our study strongly suggests that $A\beta P_{1-40}$ forms calcium-permeable, Zn^{2+}-sensitive channels in vitro and allows calcium transport across lipid membranes. Such calcium exchange across the cell plasma membrane could destabilize cellular calcium homeostasis and induce cellular toxicity.

ACKNOWLEDGMENT

We thank Drs. Seung Rhee, Arjan Quist, Ashok Parbhu, Nils Almqvist, and Rajinder Bhatia for insightful advice and suggestions. We thank Dr. Russell Rydel from Athena Neurosciences for kindly providing us with the anti-AβP antibodies and also Dr. Y. Hirakura for providing $A\beta P_{1-40}$ which was synthesized at Yale University and which was successfully reconstituted in his laboratory for recording channel activity.

REFERENCES

1. Glenner, G. G., and Wong, C. (1984) *Biochem. Biophys. Res. Commun. 120*, 885−890.
2. Masters, C. L., Multhaup, G., Simms, S., Pottgiesser, J., Martins, R. N., and Beyreuther, K. (1985) *EMBO J. 4*, 2757−2763.
3. Nashlund, J., Thyberg, J., Thernberg, L. O., Wernstedt, C., Karlstrom, A. R., Bogdanovic, N., Gandy, S. E., Lannfelt, L., Terenius, L., and Nordstedt, C. (1995) *Neuron 15*, 219−228.
4. Schendel, S. L., Xie, Z., Montal, M. O., Matsuyama, S., Montal, M., and Reed, J. C. (1997) *Proc. Natl. Acad. Sci. U.S.A. 94*, 5113−5118.
5. Antonsson, B., Conti, F., Ciavatta, A., Montessuit, S., Lewis, S., Martinou, I., Bernasconi, L., Bernard, A., Mermod, J. J., Mazzei, G., Maundrell, K., Gambale, F., Sadoul, R., and Martinou, J. C. (1997) *Science 277*, 370−372.
6. Scheuner, D., Eckman, C., Jensen, M., Song, X., Citron, M., Suzuki, N., Bird, T. D., Hardy, J., Hutton, M., Kukull, W., Larson, E., Levy-Lahad, E., Viitanen, M., Peskind, E., Poorkaj, P., Schellenberg, G., Tanzi, R., Wasco, W., Lannfelt, L., Selkoe, D., and Younkin, S. (1996) *Nat. Med. 2*, 864−870.
7. Duff, K., Eckman, C., Zehr, C., Yu, X., Prada, C. M., Perez-tur, J., Hutton, M., Buee, L., Harigaya, Y., Yager, D., Morgan, D., Gordon, M. N., Holcomb, L., Refolo, L., Zenk, B., Hardy, J., and Younkin, S. (1996) *Nature 383*, 710−713.
8. Gandy, S. E., Caporaso, G. L., Buxmaum, J. D., De Cruz Silva, O., Iverfeldt, K., Nordstedt, C., Suzuki, T., Czernik, A. J., Nairn, A. C., and Greengard, P. (1993) *Ann. N.Y. Acad. Sci. 695*, 117−121.
9. Pike, C. J., Walencewicz, A. J., Kosmoski, J., Cribbs, D. H., Glabe, C. G., and Cotman, C. W. (1995) *J. Neurochem. 64*, 253−265.
10. Price, D. L., Sisodia, S. S., and Gandy, S. E. (1995) *Curr. Opin. Neurol. 8*, 268−274.
11. Sisodia, S. S., and Price, D. L. (1995) *FASEB J. 9*, 366−370.
12. Yankner, B. A., Duffy, L. K., and Kirschner, D. A. (1990) *Science 250*, 279−282.
13. Arispe, N., Pollard, H. B., and Rojas, E. (1993) *Proc. Natl. Acad. Sci. U.S.A. 90*, 10573−10577.
14. Arispe, N., Rojas, E., and Pollard, H. B. (1993) *Proc. Natl. Acad. Sci. U.S.A. 90*, 567−571.
15. Arispe, N., Pollard, H. B., and Rojas, E. (1996) *Proc. Natl. Acad. Sci. U.S.A. 90*, 1710−1715.
16. Rhee, S. K., Quist, A. P., and Lal, R. (1998) *J. Biol. Chem. 273*, 13379−13382.
17. Zhu, Y. W., Zhang, Y., and Lal, R. (1998) *Biophys. J. 74*, A316.
18. Kosik, K. S., and Coleman, P. (1992) *Neurobiol. Aging 13*, 535−630.
19. Calingasan, N. Y., Gandy, S. E., Baker, K. F., Sheu, K. S., Kim, H. M., Wisniewski, H. M., and Gibson, G. E. (1995) *Brain Res. 677*, 50−60.
20. Benzi, G., and Moretti, A. (1995) *Neurobiol. Aging 16*, 661−674.
21. Walter, M. F., Mason, P. E., and Mason, R. P. (1997) *Biochem. Biophys. Res. Commun. 233*, 760−764.
22. Salinero, O., Moreno-Flores, M. T., Ceballos, M. L., and Wandosell, F. (1997) *J. Neurosci. Res. 47*, 216−223.
23. Li, J., Xu, M., Zhou, H., Ma, J., and Potter, H. (1997) *Cell 90*, 917−927.
24. Seilheimer, B., Bohrmann, B., Bondolfi, L., Muller, F., Stiber, D., and Dobeli, H. (1997) *J. Struct. Biol. 119*, 59−71.
25. Kim, T. W., Pettingell, W. H., Jung, Y.-K., Kovacs, D. M., and Tanzi, R. E. (1997) *Science 277*, 373−376.
26. Ito, E., Oka, K., Etcheberrigaray, R., Nelson, T. J., Mcphie, D. L., Tofel-Grehl, B., Gibson, G. L., and Alkon, D. L. (1994) *Proc. Natl. Acad. Sci. U.S.A. 91*, 534−538.
27. Mattson, M. P., Cheng, B., Davis, B., Bryant, K., Lieberburg, I., and Rydel, R. E. (1992) *J. Neurosci. 12*, 376−389.
28. Etcheberrigaray, R., Ito, E., Kim, C. S., and Alkon, D. L. (1994) *Science 264*, 276−279.
29. Bhatia, R. K., Lin, H., and Lal, R. (1999) *Biophys. J. 76*, A206.
30. Kawahara, M., Arispe, N., Kuroda, M., and Rojas, E. (1997) *Biophys. J. 73*, 67−75.
31. Mason, R. P., Estermyer, J. D., Jeremiah, F. K., and Mason, P. E. (1996) *Biochem. Biophys. Res. Commun. 222*, 78−82.
32. Durell, S. R., Guy, H. R., Arispe, N., Rojas, E., and Pollard, H. V. (1994) *Biophys. J. 67*, 2137−2145.
33. Mirzabekov, T., Lin, M. C., Yuan, W. L., Marshall, P. J., Carman, M., Tomaselli, K., Lieverburg, I., and Kagan, B. L. (1994) *Biochem. Biophys. Res. Commun. 202*, 1142−1148.
34. Hirakura, Y., Kirino, Y., and Kagan, B. L. (1998) *Biophys. J. 74*, A389.
35. Lal, R., and Proksch, R. (1997) *Int. J. Imaging Syst. Technol. 8*, 293−300.
36. Lal, R., Drake, B., Blumberg, D., Saner, D. S., Hansma, P. K., and Feinstein, S. K. (1995) *Am. J. Physiol. 269*, C275−C285.
37. Anholt, R., Fredkin, D. R., Deerinck, T., Ellisman, M., Montal, M., and Lindstrom, J. (1982) *J. Biol. Chem. 257*, 7122−7134.
38. Rhee, S. K., Bevans, C., and Harris, A. L. (1996) *Biochemistry 35*, 9212−9223.
39. Lal, R., Kim, H., Garavito, R. M., and Arnsdorf, M. F. (1993) *Am. J. Physiol. 265*, C851−C856.
40. Deamer, D. W., and Uster, P. S. (1983) in *Liposomes* (Ostro, M. J., Ed.) pp 27−51, Marcel Dekker, New York.
41. Roher, A. E., Chaney, M. O., Kou, Y.-M., Webster, S. D., Stine, W. B., Haverkamp, L. J., Woods, A. S., Cotter, R. J., Touhy, J. M., Krafft, G. A., Bonnell, B. S., and Emmerling, M. R. (1996) *J. Biol. Chem. 271*, 20631−20635.
42. Choo-Smith, L.-P., Garzon-Rodriguez, W., Glabe, C. G., and Surewicz, W. S. (1997) *J. Biol. Chem. 272*, 22987−22990.
43. Hass, C., Schlossmacher, M. G., Hung, A. G., Vigo-Pelfrey, C., Mellon, A., Ostaszewski, B. L., Lieberberg, I., Koo, E. H., Schenk, D., Teplow, D. B., and Selkoe, D. J. (1992) *Nature 359*, 322−325.
44. Seubert, P., Vigo-Pelfrey, C., Esch, F., Lee, M., Dovey, H., Davis, D., Sinha, S., Schlossmacher, M., Whaley, J., Swindlehurst, C., McCormack, R., Wolfert, R., Selkoe, D., Lieberburg, I., and Schenk, D. (1992) *Nature 359*, 325−327.
45. Shoji, M., Golde, T. E., Ghiso, J., Cheun, T. T., Estus, S., Shaffer, L. M., Cai, X.-D., Mckay, D. M., Tintner, R., Frangione, B., and Younkin, S. G. (1992) *Science 258*, 126−129.
46. Bush, A. I., Pettingell, W. H., de Paradis, M., Tanzi, R. E., and Wasco, W. (1994) *J. Biol. Chem. 269*, 26618−26621.
47. Bush, A. I., Pettingell, W. H., Multhaup, G., de Paradis, M., Vonsattel, J. P., Gusella, J. F., Beyreuther, K., Masters, C. L., and Tanzi, R. E. (1994) *Science 265*, 1464−1467.
48. Garzon-Rodriguez, W., Sepulveda-Becerra, M., Milton, S., and Glabe, C. G. (1997) *J. Biol. Chem. 272*, 21037−21044.
49. Assaf, S. Y., and Chung, S. H. (1984) *Nature 308*, 734−736.

50. Howell, G. A., Welch, M. G., and Frederickson, C. J. (1984) *Nature 308*, 736−773.
51. Lin, M.-C., Mirzabekov, T., and Kagan, B. L. (1997) *J. Biol. Chem. 272*, 44−47.
52. Hirakura, Y., and Kagan, B. L. (1999) *Biophys. J. 76*, A443.
53. Kourie, J. I. (1999) Synthetic mammalian C-type natriuretic peptide forms large cation channels, *FEBS Lett. 445*, 57−62.
54. Yang, A. J., Chandswangbhuvana, D., Margol, L., and Glabe, C. G. (1998) Loss of endosomal/lysosomal membrane impermeability is an early event in amyloidA beta 1−42 pathogenesis, *J. Neurosci. Res. 52*, 691−698.

BI982997C